J Physiol 588.14 (2010) pp 2571–2587

The Journal of Physiology

Glycinergic and GABAergic tonic inhibition fine tune inhibitory control in regionally distinct subpopulations of dorsal horn neurons

Tomonori Takazawa[1] and Amy B. MacDermott[1,2]

[1] *Department of Physiology and Cellular Biophysics and* [2] *Department of Neuroscience, Columbia University, New York, NY 10032, USA*

Inhibition mediated by glycine and GABA in the spinal cord dorsal horn is essential for controlling sensitivity to painful stimuli. Loss of inhibition results in hyperalgesia, a sensitized response to a painful stimulus, and allodynia, a pain-like response to an innocuous stimulus like touch. The latter is due, in part, to disinhibition of an excitatory polysynaptic pathway linking low threshold touch input to pain projection neurons. This critical impact of disinhibition raises the issue of what regulates the activity of inhibitory interneurons in the dorsal horn under non-pathological conditions. We have found that inhibitory neurons throughout lamina I–III, identified by the GAD67 promoter-driven EGFP, are tonically inhibited by glycine or GABA in a regionally distinct way that is mirrored by their inhibitory synaptic input. This tonic inhibition strongly modifies action potential firing properties. Surprisingly, we found that inhibitory neurons at the lamina II/III border are under tonic glycinergic control and receive synapses that are predominantly glycinergic. Futhermore, this tonic glycinergic inhibition remains strong as the mice mature postnatally. Interestingly, GlyT1, the glial glycine transporter, regulates the strength of tonic glycinergic inhibition of these glycine-dominant neurons. The more dorsal lamina I and IIo inhibitory neurons are mainly under control by tonic GABA action and receive synapses that are predominantly GABAergic. Our work supports the hypothesis that tonic glycine inhibition controls the inhibitory circuitry deep in lamina II that is likely to be responsible for separating low threshold input from high threshold output neurons of lamina I.

(Received 17 February 2010; accepted after revision 17 May 2010; first published online 24 May 2010)

Corresponding author T. Takazawa: Department of Physiology and Cellular Biophysics, Columbia University, 630 W. 168st St, Room 1109, New York, NY 10032, USA. Email: tt2225@columbia.edu

Abbreviations EGFP, enhanced green florescent protein; $GABA_AR$, $GABA_A$ receptor; GAD, glutamate decaroboxylase; GIN, GFP-expressing inhibitory neurons; GlyT1, glycine transporter 1; GlyR, glycine receptor; I_{HOLD}, holding current; I_{tGABA}, tonic inhibitory current mediated by $GABA_AR$; I_{tgly}, tonic inhibitory current mediated by GlyR.

Introduction

Sensory neurons responsive to innocuous mechanical stimuli, including heavily myelinated Aβ fibre and unmyelinated C fibre neurons, terminate near the lamina II/III border of the spinal cord. For the most part, C and lightly myelinated Aδ fibres carrying noxious, temperature and itch inputs terminate more dorsally (Light & Perl, 1979). Local circuitry acts on those sensory signals in the spinal cord dorsal horn, influencing whether they will be transmitted, via projection neurons, to higher brain centres. The local circuitry in lamina I–III is composed primarily of interneurons, 30–40% of which are immunoreactive for GABA and therefore are inhibitory. Glycine coexists in a subpopulation of the GABAergic neurons (Todd & Sullivan, 1990). These inhibitory interneurons have been proposed to function as a gate, suppressing or allowing transmission of pain or other sensory modalities to the brain (Melzack & Wall, 1965). The importance of inhibitory neurons in the dorsal horn is indicated by reports that spinal disinhibition is a powerful contributing factor in the development of sensitization to painful stimuli or hyperalgesia (Yaksh, 1989; Sivilotti & Woolf, 1994). Inhibition in the dorsal horn is also important in preventing development of painful responses to touch, a condition called allodynia (Yaksh, 1989; Sivilotti & Woolf, 1994; Sherman & Loomis, 1996; Sorkin & Puig, 1996).

Despite this critical role for inhibitory interneurons in dorsal horn function, surprisingly little is known about how their normal activity is regulated by local circuitry. Recent reports have shown that inhibitory interneurons in the dorsal horn receive inhibitory synaptic

DOI: 10.1113/jphysiol.2010.188292

inputs from other interneurons (Reinold *et al.* 2005; Labrakakis *et al.* 2009). In addition, subpopulations of inhibitory neurons receive excitatory afferent drive from high threshold (Aδ and C) peripheral fibres (Hantman *et al.* 2004; Heinke *et al.* 2004) or both low threshold (Aβ) and high threshold fibres (Daniele & MacDermott, 2009). A study of strychnine-induced allodynia in rat trigeminal neurons showed that PKCγ expressing neurons in inner lamina II (lamina IIi) are importantly involved in the allodynia and thus are normally under strong inhibitory control mediated by GlyRs (Miraucourt *et al.* 2007). This study raises the possibility that inhibition in the superficial dorsal horn, including inhibition of inhibitory interneurons, could be dependent upon the precise laminar location of the neurons involved.

Tonic inhibition has been identified as a key regulator of inhibitory tone in several brain regions (Semyanov *et al.* 2004; Farrant & Nusser, 2005). To date, studies investigating tonic inhibition in the dorsal horn have largely focused on that mediated by the $GABA_A$ receptor ($GABA_AR$) (Ataka & Gu, 2006; Takahashi *et al.* 2006; Mitchell *et al.* 2007). Tonic activation of GlyRs has not been documented in the dorsal horn of mature mice though it has been reported in juvenile rats (Mitchell *et al.* 2007). We have tested whether inhibitory neurons in the dorsal horn have tonic conductance mediated by GlyRs.

In these studies, we found that inhibitory neurons at the lamina II/III border received tonic glycinergic inhibition as well as mostly glycinergic synaptic inputs. In contrast, tonic inhibition, like the associated inhibitory synaptic activity, was most strongly mediated by $GABA_ARs$ in lamina I and IIo. Our data indicate that tonic inhibition, mediated by GlyRs and $GABA_ARs$, may be a mechanism that fine tunes output of dorsal horn inhibitory neurons in a regionally specific manner.

Methods

Spinal cord slice preparation

Mice used in this study were homozygous for a transgene that has enhanced green florescent protein (EGFP) expression controlled by the mouse *gad1* gene promoter. This gene encodes glutamate decaroboxylase (GAD) 67 (Oliva *et al.* 2000). The mice were obtained from The Jackson Laboratory (Bar Harbor, ME, USA) and interbred at our facility. Nearly all of these EGFP+ neurons in lamina I and II are GABAergic, although the proportion of GABAergic neurons found to be EGFP+ varies by study (30–70%; see Heinke *et al.* 2004; Dougherty *et al.* 2005). Postnatal mice (postnatal day (P)16 to P32) were anaesthetized with isoflurane and decapitated, and the lumbar (L3–L5) region of the spinal cord was removed in a manner approved by the Columbia University Institutional Animal Care and Use Committee. The spinal cords were initially placed in ice-cold dissection solution, then embedded in an agarose block and cut into transverse slices (400 μm) with a microtome (Leica, VT1200S). Slices were incubated in oxygenated recovery solution at 35°C for 1 h and then at room temperature for at least 1 h before recording. Slices were transferred to an upright microscope (BX51WI, Olympus) equipped with fluorescence for identification of positive neurons and IR-DIC for electrophysiological recordings. Slices were continuously perfused with oxygenated Krebs solution at a low flow rate of 2 ml min^{-1}. Recordings were made at 32 ± 1°C. Krebs recording solution saturated with 95% O_2–5% CO_2 had the following composition (in mM): 125 NaCl, 2.5 KCl, 1.25 NaH_2PO_4, 26 $NaHCO_3$, 25 glucose, 1 $MgCl_2$, 2 $CaCl_2$, pH 7.4. Recovery solution was the same as the recording solution but with 1.5 mM $CaCl_2$ plus 6 mM $MgCl_2$. Dissection solution was the same as recovery solution but with 1 mM kynurenic acid added.

Patch-clamp recording

Whole-cell patch recordings were made from inhibitory EGFP+ neurons. Recording electrodes with a resistance of 3–5 MΩ were pulled from borosilicate glass capillaries (0.86 mm ID, 1.5 mm OD) using a P97 electrode puller (Sutter Instrument Co., Novato, CA, USA). Intracellular solution had the following composition (in mM): 120 caesium methanesulfonate, 10 sodium methanesulfonate, 10 EGTA, 1 $CaCl_2$, 10 Hepes, 5 lidocaine *N*-ethyl bromide quaternary salt-Cl, 0.5 NaGTP, 5 MgATP, pH adjusted to 7.2 with CsOH, osmolarity 280 mosmol l^{-1} (for voltage-clamp), 120 potassium methanesulfonate, 10 NaCl, 10 EGTA, 1 $CaCl_2$, 10 Hepes, 0.5 NaGTP, 5 MgATP, pH adjusted to 7.2 with KOH, osmolarity 280 mosmol l^{-1} (for current-clamp). Given the $[Cl^-]$ of Krebs solution and the intracellular solution for voltage- and current-clamp, the Cl^- equilibrium potential was −74 mV and −61 mV, respectively. Junction potential was corrected before recording. We always waited at least 5 min after membrane rupture to obtain a stable recording.

Because the pipette solution for voltage clamp experiments was caesium methanesulfonate with a low final concentration of chloride, $GABA_AR$ and GlyR-mediated currents at 0 mV were outward. In addition, most potassium currents were blocked and glutamate receptor-mediated currents were at reversal potential. Recordings were made from 129 EGFP+ neurons located in lamina I–III under voltage-clamp control at 32°C. Among the 129 neurons, 61 were judged to be adequate for further analysis based on the following criteria: input resistance >350 MΩ, access resistance <40 MΩ and stable recording for sufficient duration (>25 min).

We recorded from 127 EGFP+ neurons located in lamina I–III under current-clamp conditions at 32°C. Among these recordings, 61 neurons were judged to be adequate for physiological characterization based on the following criteria: resting membrane potential was more negative than −50 mV, input resistance >250 MΩ, action potentials overshoot 0 mV, and stable recording for sufficient duration (>10 min).

Data were recorded and acquired using an Axopatch 200B amplifier and pCLAMP 9 software (Molecular Devices, Sunnyvale, CA, USA). Data were filtered at 2 kHz and digitized at 10 or 20 kHz. After the recording was completed, images of the recorded neurons were taken using a CCD camera and stored by Scion Image (Scion Corp., Frederick, MD, USA). These images were used to document the laminar location of the neuron studied. Under IR-DIC optics, lamina II appears translucent. If the cell body of the neuron was within this translucent area, it was judged to be in lamina II. Neurons located in lamina II were further divided into IIi and IIo based on the images. If a neuron was just dorsal or ventral to the translucent band, it was considered to be in lamina I or III, respectively. The distance between the centre of soma and the border of the white and grey matter for most recorded neurons was also measured to make sure there was a clear distinction among the sample of cells belonging to different laminae (Chery & de Koninck, 1999). The average distances for neurons obtained from mice during their 3rd postnatal week (3W) located in lamina I, IIo, IIi and III were (μm): 12 ± 3 ($n = 14$), 46 ± 3 ($n = 30$), 93 ± 4 ($n = 33$), and 131 ± 13 ($n = 6$), respectively. The distances for neurons obtained from mice during their 5th postnatal week (5W) in lamina I, IIo, IIi, and III were (μm): 17 ± 3 ($n = 4$), 48 ± 4 ($n = 11$), 97 ± 11 ($n = 11$), and 110 ($n = 1$), respectively.

Data analysis

mIPSCs were detected and analysed using Mini Analysis software (Synaptosoft, Inc., Decatur, GA, USA) off-line. The threshold for detection of mIPSCs was set at three times the root mean square of the background noise, and each event was further confirmed by visual inspection after detection. Two criteria, the decay τ values of mIPSCs and the effect of bicuculline on mIPSC frequency, were used to divide EGFP+ neurons into two distinct populations. The decay τ values of mIPSCs were defined as the time required for each event to decay by 67% and the mean τ value was calculated by averaging the decay τ values of individual events during a 2 min window in the presence of TTX. For calculating the effect of bicuculline on mIPSC frequency, the number of mIPSCs counted within the last 2 min in the presence of TTX and bicuculline was divided by the number of mIPSCs counted within a 2 min window just before bicuculline application.

Charge transfer associated with mIPSCs (Q_{SC}) in a given time period (t) was calculated using the equation $Q_{SC} = F_m \times Q_{mIPSCs} \times T$, where F_m is the frequency (Hz) of mIPSCs, Q_{mIPSCs} is the average charge transfer per mIPSC during a 2 min window, and T is the duration of window. The charge transfer associated with tonic currents (Q_{TC}) was calculated according to the equation: $Q_{TC} = I_{TC} \times T$, where Q_{TC} is the charge transfer produced by tonic currents, I_{TC} is the tonic current amplitude, calculated as the difference in the averaged holding current before and after drug application. For calculating averaged holding current, mIPSCs were excluded by software (written by Yukio Koyama) to avoid any distortion by mIPSCs. To accomplish this exclusion, threshold for detection of mIPSCs was set at three times the root mean square of the background noise. Each event was further confirmed by visual inspection to ensure a complete match with events already detected by Mini Analysis. Points from 10 ms before and to 150 ms after the peak of mIPSCs were excluded from analysis. Most mIPSCs decayed to baseline 150 ms after the peak. After removing mIPSCs, all-point histograms were plotted for each window and fitted to a Gaussian curve. The mean of the fitted Gaussian was considered to be the mean holding current. Standard deviations of holding currents (S.D. of I_{HOLD}) were calculated after excluding mIPSCs according to the formula:

$$\text{S.D.}^2 = \sum_{i=1}^{N} (Ci - m)^2 / N - 1$$

where N is the number of samples per window, Ci is the I_{HOLD} at sample i, and m is the mean I_{HOLD}.

To estimate I_{TC} density, measured I_{TC} amplitude was normalized by membrane capacitance, which was obtained by integrating the area under the transient capacitive phase of the current response to a 5 mV depolarizing step pulse in voltage-clamp mode.

Action potentials were analysed using AxoGraph X software (AxoGraph Scientific, Sydney, Australia). Rheobase was defined as the current step magnitude required for the minimum number of action potentials. To calculate the current amplitude required for 20 Hz action potentials, the relationship between output firing frequency (F) and input current (I) was fitted by either a linear equation: $F(X) = KX - A$, or a single exponential equation: $F(X) = K\ln(X - C) - A$, where F is firing frequency, X is injected current amplitude, K is gain, A is offset and C is the shift in offset.

EGFP+ neurons obtained from 3W mice ($n = 55$, range; P16–18, mean; P16.7 ± 0.5) were grouped into populations with different firing patterns, which have distinct membrane properties (Supplemental Fig. 1 and

Supplemental Table 1). These firing patterns are consistent with past reports using GFP-expressing inhibitory neuron (GIN) mice, although the incidence of neurons exhibiting specific firing patterns varies among studies (Heinke *et al.* 2004; Dougherty *et al.* 2005; Daniele & MacDermott, 2009). Although we observed gap-firing neurons in this current study as well as our previous study (Daniele & MacDermott, 2009), we included them in the delayed-firing neuron group because both gap- and delayed- firing neurons have A-type K+ current (Heinke *et al.* 2004). Also, they are a minor population even after combining them into one group. Single-spike neurons were excluded from further analysis, because they did not fire tonically even after large current injection (>200 pA, Supplemental Fig. 1*D*). Because single-spike neurons were also a minor population (<10% of total), our sampling procedure should be representative of most inhibitory neurons in the dorsal horn.

Drug application

We used bicuculline methobromide as a $GABA_AR$ antagonist unless otherwise indicated for the following reasons. First, it has been reported that bicuculline blocks tonic inhibitory currents mediated by $GABA_ARs$ (I_{tGABA}) in lamina II of the spinal cord (Ataka & Gu, 2006; Takahashi *et al.* 2006). Second, an optimal concentration of SR95531 (SR), the other $GABA_AR$ antagonist widely used for blocking I_{tGABA}, varies among studies (Brickley *et al.* 2001; Stell & Mody, 2002; Yeung *et al.* 2003), probably due to a difference of $GABA_AR$ subtypes responsible for tonic currents in distinct CNS regions (Semyanov *et al.* 2004; Farrant & Nusser, 2005). Nevertheless, we used SR for a subset of current-clamp experiments. SR (30 μM) had only a small effect (~20%) on evoked glycinergic IPSCs recorded from motoneurons (Beato, 2008), suggesting that using over 30 μM could make it difficult to distinguish the effect of SR on $GABA_ARs$ and GlyRs. Therefore, we chose 30 μM to maximize the effect of SR on $GABA_ARs$ with minimal effects on GlyRs. 1,2,3,4-Tetrahydro-6-nitro-2,3-dioxo-benzo[f]quinoxaline-7-sulfonamide (NBQX) (10 μM; Ascent Scientific, Avonmouth, UK), D-2-amino-5-phosphonovalerate (D-AP5) (50 μM; Tocris Bioscience, Ellisville, MO, USA), bicuculline methobromide (10 μM; Ascent Scientific), SR95531 (30 μM; Ascent Scientific), and strychnine hydrochloride (1 μM; Sigma-Aldrich) were prepared as 1000× concentrated frozen stock solution aliquots. TTX (0.5 μM; Ascent Scientific) and ORG 24598 (10 μM; Sigma-Aldrich) were prepared as 2000× and 500× concentrated frozen stock solution aliquots, respectively. To avoid any transition in F or I_{HOLD} during the analysis period that is not related to the drug effect, each drug was applied for 10 min to obtain a steady state.

Statistics

Results are presented as means ± S.E.M. Statistical tests were performed using GraphPad Prism software (GraphPad Software Inc., La Jolla, CA, USA). Differences between groups are considered significant for $P < 0.05$.

Results

Disinhibition results in increased excitability of EGFP+ neurons

The impact of endogenously released glycine and GABA on the excitability of inhibitory interneurons was determined by testing the effect of receptor blockade on action potential firing of EGFP+ inhibitory neurons. Injected current steps were used to induce trains of action potentials and were applied using a pipette solution providing a physiological Cl^- gradient ($E_{Cl} = -61$ mV). Under control conditions, the majority of cells fired repetitive action potentials and were classified as tonic or delayed firing neurons (see Methods; Supplemental Fig. 1). Frequency of firing increased with amplitude of injected current (Fig. 1*A*). The number of evoked action potentials (output firing frequency, F) was plotted as a function of amplitude of the depolarizing current pulses (I; 0 up to ~240 pA, 1 s duration). Curves for F–I relationships were drawn for individual cells as shown in Fig. 1*B* and then were combined as in Fig. 1*C* ($n = 11$). Data obtained from neurons located in lamina I–III (lamina I, $n = 2$; IIo, $n = 3$; IIi, $n = 5$; III, $n = 1$), excluding single-spike neurons (Supplemental Fig. 1), were pooled for drawing the combined curve. When the current injection protocol was repeated in the presence of the $GABA_AR$ antagonist bicuculline (10 μM), the F–I curve shifted left. When the GlyR antagonist strychnine (1 μM) was subsequently added to the bath together with bicuculline, the F–I curve shifted still further to the left. These results indicate that endogenously released glycine and GABA depressed neuronal excitability.

Bicuculline was always applied before strychnine throughout this study because strychnine is less selective for GlyRs than bicuculline is for $GABA_ARs$ (Jonas *et al.* 1998). Specifically, in a study on neonatal rat motor neurons, 1 μM strychnine was found to block 100% of the current activated by glycine. Bicuculline at 10 μM blocked less that 10% of glycine activated current and all of the GABA activated current (Jonas *et al.* 1998). Using this approach of applying GlyR and $GABA_AR$ antagonists, we found that endogenous glycine and GABA influence the excitability of inhibitory neurons.

There were additional indications that endogenously released glycine and GABA normally suppress excitability of inhibitory interneurons. Threshold for action potential

initiation (rheobase) was decreased in the presence of bicuculline plus strychnine compared to control and in the presence of bicuculline (Fig. 1*D*; $n = 11$, one-way ANOVA with Tukey's *post hoc* test). Moreover, the current amplitude required to drive action potentials at 20 Hz (see Methods) was decreased in the presence of bicuculline and bicuculline plus strychnine (Fig. 1*E*; $n = 11$, one-way ANOVA with Tukey's *post hoc* test). These results show that blockade of GlyR- and $GABA_A$R-mediated conductances in inhibitory neurons caused enhanced excitability, suggesting that these conductances normally provide modulatory control of the inhibitory tone in the local circuits.

A potentially confounding factor in interpreting the actions of bicuculline as being mediated by $GABA_A$ receptors is that bicuculline has been shown to block small-conductance Ca^{2+}-activated potassium channels (SK channels) (Seutin *et al.* 1997; Debarbieux *et al.* 1998; Khawaled *et al.* 1999). Because the activity of SK channels is responsible for slow afterhyperpolarizations (AHP) following action potentials in many excitable cells, bicuculline could modify cell excitability through SK channel inhibition. We used SR95531 as a specific $GABA_A$R antagonist that does not act on SK channels (Heaulme *et al.* 1987) to confirm whether blockade of $GABA_A$R-mediated conductances rather than SK channels caused enhanced excitability (Supplemental Fig. 2, $n = 6$). SR95531 (30 μM) shifted the *F–I* curve left as did bicuculline (Supplemental Fig. 2*B*) with decreasing rheobase (Supplemental Fig. 2*C*, $P < 0.01$, paired *t* test). SR95531 also decreased the current amplitude required to drive action potentials at 20 Hz (Supplemental Fig. 2*D*, $P < 0.05$, paired *t* test). These results suggest that blockade of $GABA_A$Rs without the involvement of SK channels is sufficient to enhance the excitability of inhibitory neurons.

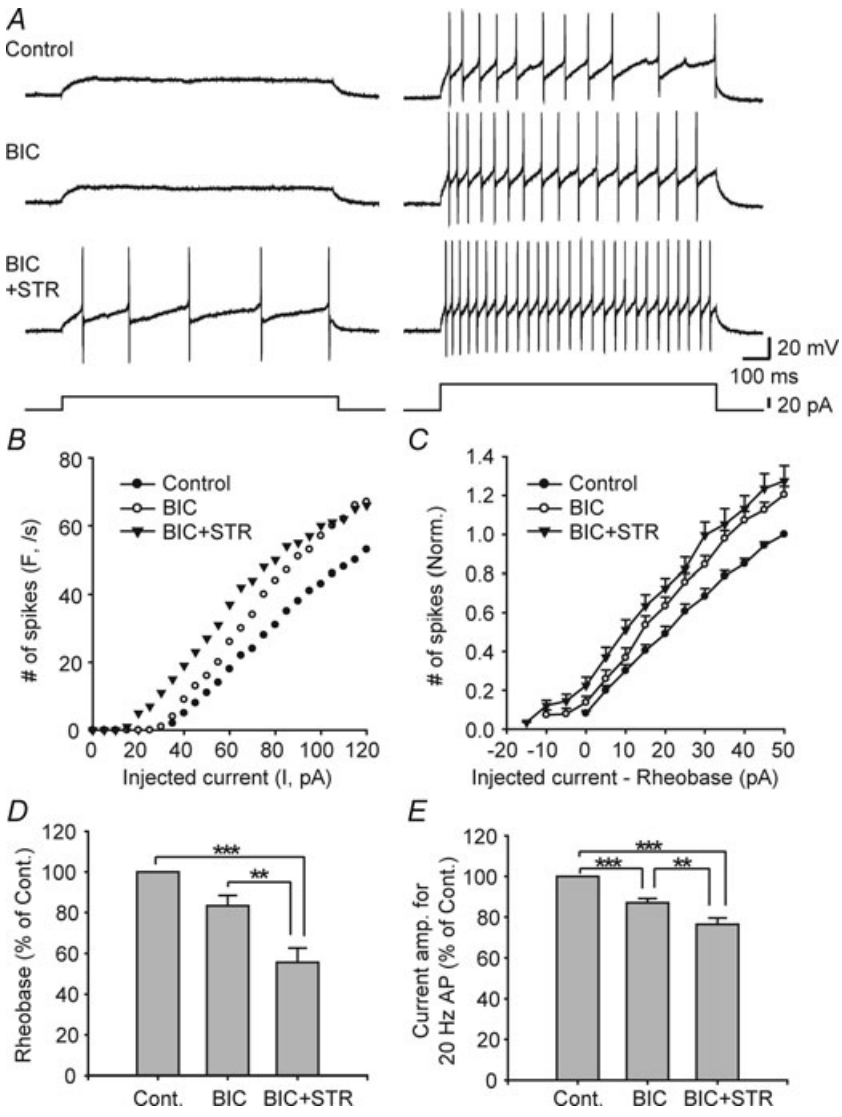

Figure 1. Effect of glycinergic and GABAergic inhibition on EGFP+ cell excitability
A, typical examples of action potentials induced by current injection (25 pA, left panel; 50 pA, right panel) under 3 conditions ((1) Control: NBQX (10 μM) and AP5 (50 μM); (2) BIC: NBQX, AP5 and bicuculline (10 μM); (3) BIC+STR: NBQX, AP5, bicuculline and strychnine (1 μM)). Resting membrane potential was kept at –65 mV. Bottom traces show injected currents. *B*, output firing frequency (*F*) over 1 s and input current (*I*) relationship under 3 conditions corresponding to *A*. *C*, *F–I* relationship of EGFP+ neurons ($n = 11$). Because rheobase (current step magnitude required for minimum number of action potentials) is variable among cells, the number of action potentials was normalized by the number of action potentials counted after stimulation with a current step 50 pA greater than rheobase under control condition to combine *F–I* relationship of every neurons. *D*, rheobase was decreased under BIC+STR condition compared to control and BIC condition ($n = 11$). *E*, current amplitude required for action potential firing at 20 Hz was decreased under BIC and BIC+STR condition compared to control, and between BIC and BIC+STR condition ($n = 11$). Data are shown as means ± S.E.M. $^{**}P < 0.01$, $^{***}P < 0.001$.

Two distinct populations of EGFP+ neurons defined by synaptic inhibitory inputs

Endogenous inhibitory control of inhibitory interneuron firing properties could be mediated by synaptic or tonic inhibition acting through GlyRs, $GABA_A$Rs or some combination of these possibilities. The EGFP+ neurons in the dorsal horn of GIN mice are known to be heterogeneous in their neurochemistry, afferent inputs and firing properties (Heinke *et al.* 2004; Dougherty *et al.* 2005; Daniele & MacDermott, 2009) and thus may also be heterogeneous in how their excitability is regulated. To determine whether different subpopulations of inhibitory neurons are regulated differently by inhibition, we used miniature inhibitory postsynaptic currents (mIPSCs) to investigate the type of inhibitory synaptic input received by EGFP+ neurons in lamina I–III obtained from animals during their 3rd postnatal week (3W) ($n = 34$, range; P16–18, mean; P16.6 ± 0.1). The neurons were voltage-clamped at 0 mV for recording mIPSCs.

Based on synaptic inhibitory input properties, including mean decay τ of mIPSCs and the effect of bicuculline on mIPSC frequency, EGFP+ neurons were readily divided into two distinct populations, either glycine-dominant (Gly-d) or GABA-dominant (GABA-d). Gly-d neurons ($n = 17$) had mIPSCs with relatively fast decay τ values, where τ is defined as the time to decay by 67%, and low sensitivity to bicuculline (Fig. 2*A*, *B* and inset in 2*E*). In contrast, GABA-d neurons ($n = 17$) had mIPSCs with relatively slow decay τ values and high sensitivity to bicuculline (Fig. 2*C*, *D* and inset in *E*). Gly-d neurons had decay τ values <13 ms while GABA-d neurons were defined as having mIPSC decay τ values >13 ms (Fig. 2*E*). Neurons with <76% decrease in frequency were considered Gly-d neurons while >76% decrease of mIPSC frequency in bicuculline were considered to be GABA-d neurons (Fig. 2*E*). The two criteria of decay τ and bicuculline sensitivity of mIPSC frequency independently separated the same two populations of neurons. In Gly-d neurons, the mean decay τ after bicuculline application was faster than that of control (Fig. 2*F*; $n = 17$, $P < 0.01$, paired t test). The simultaneous effects of bicuculline to decrease mIPSC frequency and decrease decay τ indicates that both effects are due to the action of bicuculline blocking $GABA_A$Rs.

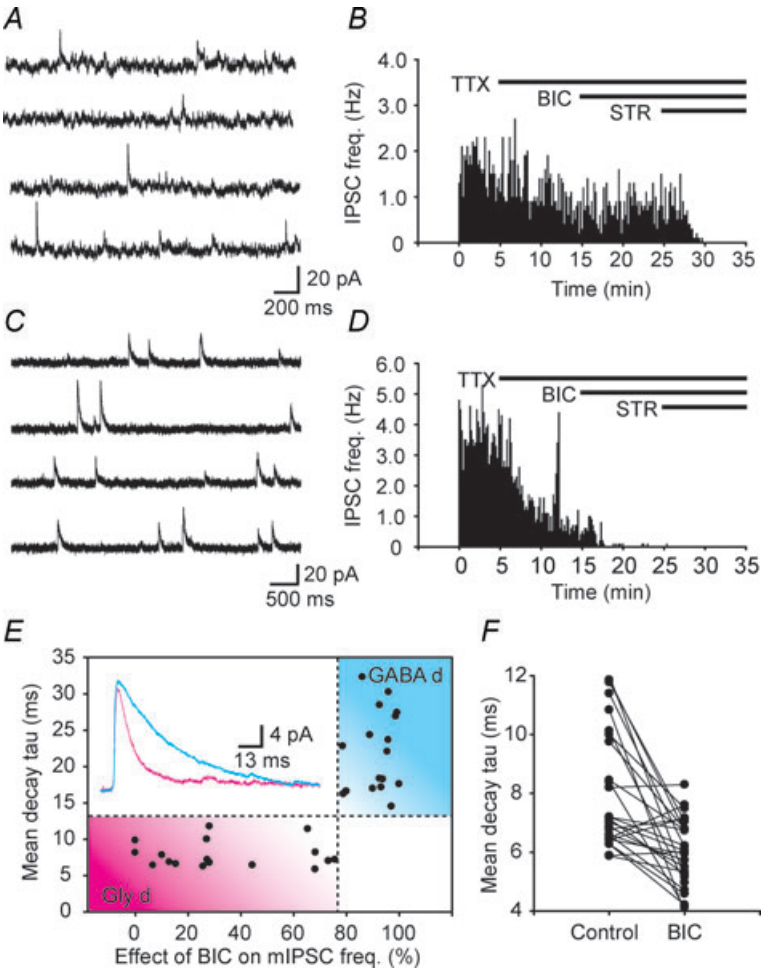

Figure 2. Two distinct types of mIPSCs recorded from different EGFP+ neurons in the dorsal horn
A and *C*, representative current traces obtained from a neuron in the presence of TTX that later was observed to have bicuculline (10 μM) resistant mIPSCs with relatively fast kinetics (*A*), and a neuron that later was observed to have bicuculline (10 μM) sensitive mIPSCs with relatively slow kinetics (*C*). Holding membrane potentials was 0 mV. *B* and *D*, histograms of mIPSC frequency as a function of time corresponding to *A* and *C*. *E*, EGFP+ neurons could be divided into two distinct populations, glycine or GABA-dominant. Glycine-dominant neurons (Gly-d, $n = 17$) were defined as having mIPSC decay τ values <13 ms while GABA-dominant neurons (GABA-d, $n = 17$) had decay τ values >13 ms. A <76% decrease of mIPSC frequency in bicuculline was considered to be Gly-d while >76% was GABA-d. Inset compares averaged mIPSCs of Gly-d (pink trace; decay $\tau = 8.4$ ms, averaged from 92 events in same neuron as *A* and *B*) and GABA-d (blue trace; decay $\tau = 26.9$ ms, averaged from 78 events in same neuron as *C* and *D*). *F*, mIPSC decay τ values of Gly-d neurons decreased after bicuculline application ($n = 17$). We measured decay τ values of individual events first and then calculated mean decay τ for each cell by averaging.

The presence of two separate populations of neurons apparent in Fig. 2*E* supports the idea that grouping EGFP+ neurons by these criteria as Gly-d and GABA-d is an effective way to functionally identify these neuronal subpopulations without including the details of minor contributions of transmitters to single mIPSCs. In addition, Gly-d neurons have significantly larger average cell capacitance (59 ± 5 pF) than GABA-d neurons (44 ± 4 pF; $P < 0.05$, unpaired t test), suggesting that cell size was greater in Gly-d than GABA-d neurons. This is also consistent with the interpretation that Gly-d and GABA-d neurons are two distinct populations of inhibitory neurons.

EGFP+ neurons located in different regions of the superficial dorsal horn have distinct properties of synaptic inhibitory inputs

The identification of two populations of inhibitory neurons based on synaptic input raises the question of whether these neurons have distinct locations within the dorsal horn or are mixed randomly throughout lamina I–III. Therefore the location of each neuron categorized as Gly-d and GABA-d was plotted as in Fig. 3*A*. From visual inspection, it is evident that Gly-d neurons are located somewhat deeper in the superficial dorsal horn while GABA-d neurons are generally located more superficially. To quantify the distribution of Gly-d and GABA-d neurons, the percentage of each type of neuron located in lamina I and IIo (lamina I–IIo) and in lamina IIi and at the dorsal border of III (lamina II/III border) is plotted in Fig. 3*B*. It is clear that EGFP+ Gly-d neurons (grey bars) were the major population at the lamina II/III border ($n = 15$) while EGFP+ GABA-d neurons (black bars) were the major population in lamina I–IIo ($n = 19$; $P < 0.01$, Fisher's exact test).

We next asked whether region specificity of synaptic inhibitory input changes developmentally, because dramatic changes have been reported in the proportions of mIPSCs that are mediated by GlyRs and $GABA_A$Rs recorded from unidentified neurons during the first 30 postnatal days in rats (Keller *et al.* 2001). The mature receptor configuration by P30 and older in those earlier rat studies was that in lamina I, mIPSCs were mediated by only GlyRs, and in lamina II mIPSCs were predominantly either only GlyRs or only $GABA_A$Rs (Chery & de Koninck, 1999; Keller *et al.* 2001). We recorded inhibitory inputs to EGFP+ inhibitory neurons obtained from animals during their 5th postnatal week (5W) ($n = 23$, range; P29–32, mean; P30.0 $\pm$ 0.2). Again, those neurons could be divided into two distinct populations based on synaptic inhibitory input properties using the same definition as neurons obtained from 3W animals. By 5 weeks, separation of Gly-d and GABA-d neurons by location was even more robust (Fig. 3*C* and *D*). In contrast to the observations by Keller *et al.* (2001), Gly-d neurons (grey bars) were prominent at the lamina II/III border ($n = 12$) and GABA-d neurons (black bars) were a major population in lamina I–IIo ($n = 11$; Fig. 3*C* and *D*; $P < 0.001$, Fisher's exact test), suggesting that region specificity of synaptic inhibitory input onto EGFP+ inhibitory neurons was preserved and even more pronounced after maturation was complete.

Tonic glycine and $GABA_A$ receptor-mediated conductances in EGFP+ neurons

Tonic inhibition, an important regulator of neuronal excitability mediated by GlyRs (Mitchell *et al.* 2007) and

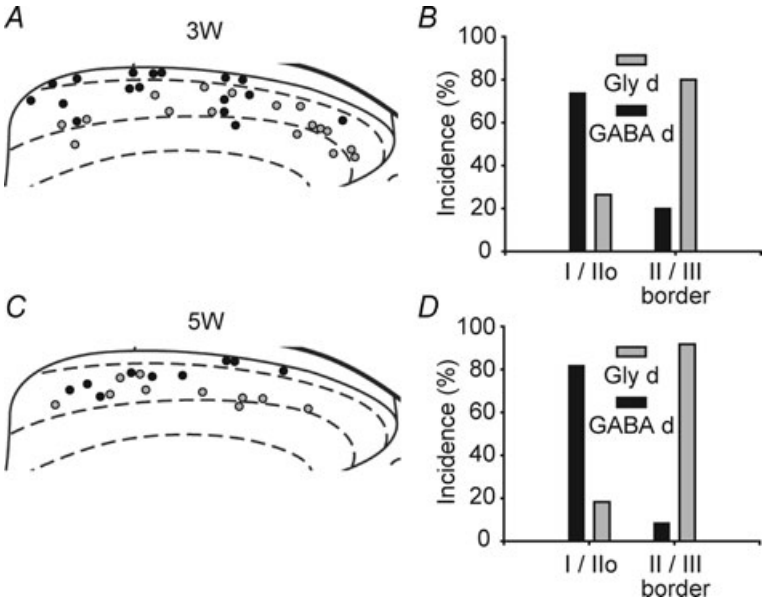

Figure 3. EGFP+ neurons have regionally distinct properties of synaptic inhibitory input
A and *C*, soma locations of Gly-d (grey circles) and GABA-d (black circles) neurons at P16–18 (3W; *A*) and at P29–32 (5W; *C*). Right and upper side of the schematic diagram shows lateral and dorsal edges of the dorsal horn, respectively. Lamina I, II, and III are separated by dotted lines. *B* and *D*, in both populations corresponding to *A* and *C*, Gly-d neurons were the major population at the lamina II/III border (3W; $n = 15$, 5W; $n = 12$), while GABA-d neurons (black bars) were the major population in lamina I and IIo (3W; $n = 19$, 5W; $n = 11$). Bars indicate incidence of neurons located at lamina I and IIo, and at lamina II/III border.

$GABA_A$Rs (Ataka & Gu, 2006; Takahashi *et al.* 2006; Mitchell *et al.* 2007), has been reported for unidentified neurons in the dorsal horn. However, tonic conductance mediated by GlyRs in the mature dorsal horn is uncertain (Mitchell *et al.* 2007). Therefore, we investigated tonic inhibition of Gly-d and GABA-d EGFP+ inhibitory neurons. When the holding current was analysed with mIPSCs excluded (see Methods), both bicuculline and strychnine produced inward shifts of mean holding currents (I_{HOLD}; Fig. 4*A* and *B*). The mIPSC frequency in both Gly-d and GABA-d neurons was on the order of 1 Hz (Table 1) in these EGFP+ neurons, making changes in I_{HOLD} straightforward to observe and calculate. For example, Fig. 4*A* and *C* show changes in both synaptic activity and I_{HOLD} at a compressed time base on top and samples at a faster time base below. Similar to Gly-d neurons, both bicuculline and strychnine produced inward shifts of I_{HOLD} in GABA-d neurons (Fig. 4*C* and *D*). Both Gly-d ($n = 7$) and GABA-d ($n = 11$) neurons showed significant inward shifts of I_{HOLD} under bicuculline and bicuculline plus strychnine conditions.

Shifts of I_{HOLD} were considered to be tonic GlyR- and $GABA_A$R-mediated currents (I_{tgly} and I_{tGABA}) for the following reasons. First, antagonist block of I_{HOLD} was always accompanied by a decrease in standard deviation of holding currents (S.D. of I_{HOLD}; see Methods) in both Gly-d and GABA-d neurons (Fig. 4*E*, one-way ANOVA with Tukey's *post hoc* test) as shown previously in hippocampal and magnocellular neurons (Bai *et al.* 2001; Park *et al.* 2006). In other words, because tonic current was mediated by a transmitter gated channel, receptor blockade produced both a decrease in channel noise and a decrease in total current. S.D. of I_{HOLD} appears to be a sensitive indicator of the level of channel activity (Mtchedlishvili & Kapur, 2006). Indeed, the decreases in I_{HOLD} and S.D. of I_{HOLD} in the presence of bicuculline and bicuculline plus strychnine were correlated (Fig. 4*F*; $n = 18$, BIC: $R = 0.53$, $P < 0.05$; BIC+STR: $R = 0.67$, $P < 0.01$; Pearson's linear regression), arguing that the decrease in I_{HOLD} was caused by blockade of $GABA_A$Rs and/or GlyRs. Second, contamination of the conductance in I_{HOLD} with activity from other channels such as AMPA and NMDA receptors is not likely because the recorded neurons were voltage-clamped at 0 mV, the same voltage as the reversal potential of those receptors. Third, shift of I_{HOLD} did not reflect many mIPSCs added together in the control condition. Given the observed frequency of mIPSCs (Table 1), summation of multiple mIPSCs is not expected to affect I_{HOLD} (see lower panel in Fig. 4*A* and *C*).

Because Gly-d neurons receive mIPSCs that are mainly glycinergic and GABA-d neurons receive mIPSCs that are mainly GABAergic, we expected that Gly-d neurons would have a stronger I_{tgly} and GABA-d neurons would have a stronger I_{tGABA}. However, the amplitude of I_{tGABA} was not different between Gly-d and GABA-d neurons (Fig. 4*G*). On the other hand, the amplitude of I_{tgly} in Gly-d neurons was greater than that in GABA-d neurons (Fig. 4*G* left columns, $P < 0.05$, unpaired *t* test). After calculating I_{tgly} and I_{tGABA} current density by dividing by cell capacitance, however, neither I_{tgly} nor I_{tGABA} was different between Gly-d and GABA-d neurons (Fig. 4*G* right columns).

The robust expression of I_{tgly} in both Gly-d and GABA-d neurons was somewhat surprising. To probe for the possible source of ambient glycine, we directly tested whether tonic GlyR-mediated conductance correlates with the amount of basal synaptic release of glycine. Amplitudes of I_{tgly} were plotted against basal glycinergic mIPSC frequencies on a cell by cell basis. Amplitudes of I_{tgly} after bicuculline application were not correlated with the glycinergic mIPSC frequency (Fig. 4*H*, $n = 18$, $R = 0.12$, $P = 0.63$, Pearson's linear regression). This was also true for S.D. of I_{HOLD} (Supplemental Fig. 3*A*; $R = 0.36$, $P = 0.16$, Pearson's linear regression). These results suggest that the tonic inhibitory conductance mediated by glycine in EGFP+ neurons is not directly dependent on synaptic inhibitory inputs.

Tonic glycine currents were significantly enhanced by a glycine transporter 1 inhibitor in EGFP+ neurons

The observation that I_{tgly} was significantly greater in Gly-d neurons than in GABA-d neurons before normalization by cell capacitance but not after normalization raises the possibility that the glycine transporter responsible for controlling extracellular glycine, glycine transporter 1 (GlyT1) (Gomeza *et al.* 2003), is just on the edge of being able to slow or prevent synaptic glycine from accumulating extrasynaptically. In other words, extracellular glycine concentration may be slightly elevated near Gly-d neurons but it would be even higher without the strong action of GlyT1. To test this possibility, we investigated I_{tgly} following exposure of spinal cord slices to ORG 24598 (ORG; 10 μM), a specific GlyT1 inhibitor. While recording from Gly-d neurons in the presence of TTX (0.5 μM) and bicuculline (10 μM), application of ORG led to an outward shift in I_{HOLD} that peaked around 5 min after application (Fig. 5*A* and *B*). Similarly, in GABA-d neurons, ORG caused an outward shift in I_{HOLD} having a comparable time course to Gly-d neurons (Fig. 5*C* and *D*). In both cases, ORG induced shifts in I_{HOLD} were blocked by strychnine.

These shifts in I_{HOLD} are believed to originate from rapid accumulation of glycine in the extracellular space that in turn enhances I_{tgly} for the following reasons. First, ORG induced changes in I_{HOLD} were not accompanied by apparent changes in mIPSC amplitude ($n = 4$, $P = 0.73$, one-way ANOVA) or frequency ($n = 4$, $P = 0.92$, one-way ANOVA), indicating that the current was not a summation of mIPSCs but was attributable to continuous GlyR

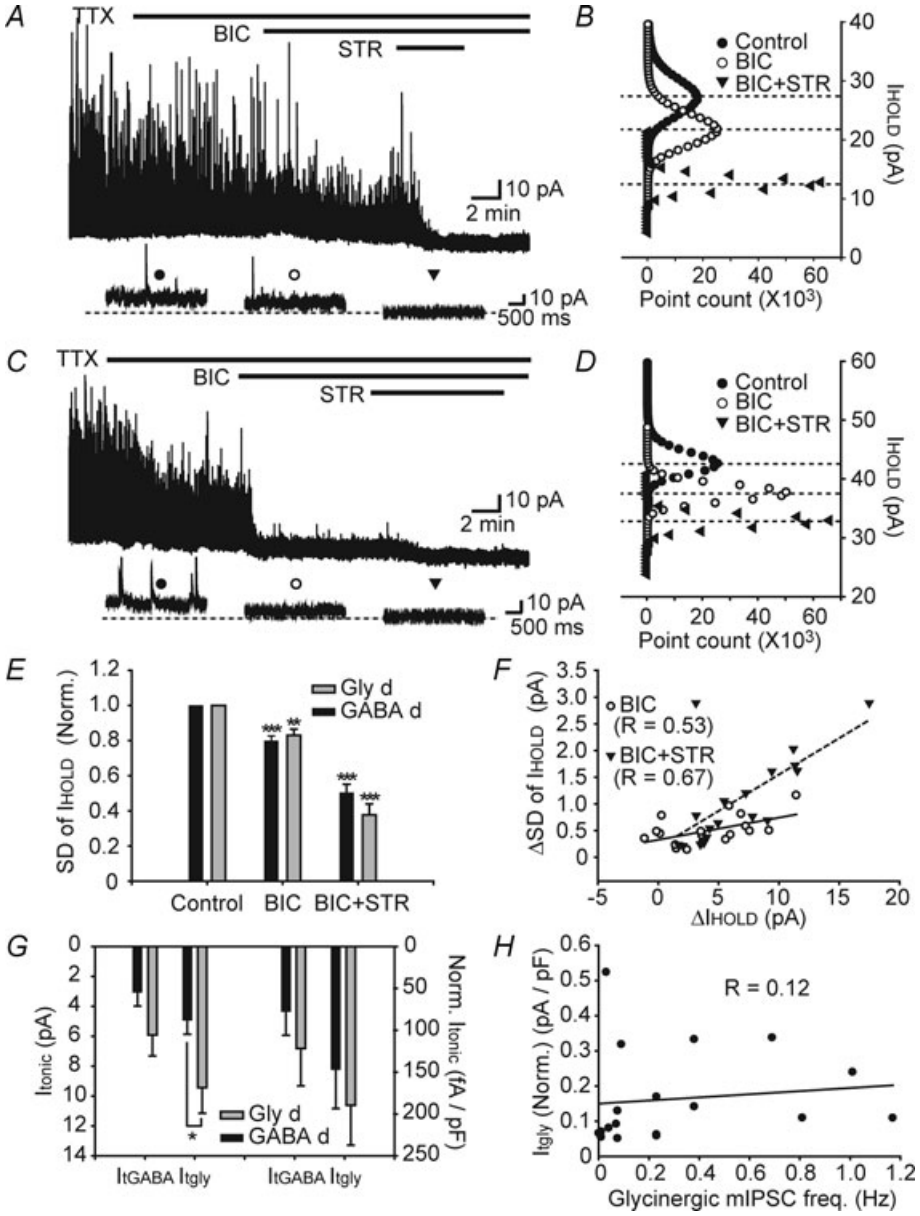

Figure 4. Tonic glycinergic and GABAergic currents in Gly-d and GABA-d EGFP+ neurons recorded from 3W mice

A and *C*, upper traces show bicuculline (BIC) and bicuculline plus strychnine (BIC+STR) induced baseline shift in Gly-d (*A*) and GABA-d neurons (*C*). Expanded time scale traces in lower panel show the shift of holding current (I_{HOLD}) under control (left), BIC (middle), and BIC+STR (right) conditions. Dotted line indicates I_{HOLD} under BIC+STR conditions. Holding membrane potentials were 0 mV. *B* and *D*, all-points histograms comparing the amplitude of I_{HOLD} under 3 conditions were constructed from 2 min recording segments from which mIPSC events were excised. Mean values for I_{HOLD} (dotted lines) were determined from Gaussian fits. Tonic current amplitude was calculated from the shift of the mean I_{HOLD} under each condition. *E*, standard deviation of holding current (S.D. of I_{HOLD}) decreased after BIC and BIC+STR application in GABA-d ($n = 11$) and Gly-d ($n = 7$) neurons. Only statistical differences between subsequent conditions are shown (Tukey's *post hoc* test). *F*, decrease in S.D. of I_{HOLD} and in I_{HOLD} after BIC (open circles and black line) and BIC+STR (filled triangles and dotted line) application were correlated ($n = 18$). *G*, both Gly-d neurons ($n = 7$, grey bars) GABA and d ($n = 11$, black bars) showed I_{tgly} and I_{tGABA}. Left columns, averaged tonic current; right columns, averaged tonic current normalized by cell capacitance. *H*, I_{tgly} was not correlated with glycinergic mIPSC frequency ($n = 18$). Data are shown as means ± S.E.M. $^{*}P < 0.05$, $^{**}P < 0.01$, $^{***}P < 0.001$.

Table 1. Synaptic inhibition on the mouse EGFP+ dorsal horn neurons

Age	Glycine/GABA	*n*	Frequency (Hz)	Amplitude (pA)
3W	Glycine-dominant	17	0.7 ± 0.1	21.8 ± 1.6
	GABA-dominant	17	1.0 ± 0.3	19.7 ± 1.5
5W	Glycine-dominant	13	0.3 ± 0.1	26.3 ± 3.0
	GABA-dominant	10	0.7 ± 0.3	22.7 ± 1.5

activation by endogenous glycine. Second, the outward shifts in I_{HOLD} were accompanied by a significant increase in S.D. of I_{HOLD} in Gly-d neurons 5 min after application of ORG (Fig. 5*E*, $n = 4$, $P < 0.05$, Tukey's *post hoc* test), and the amount of increase in I_{HOLD} and S.D. of I_{HOLD} were correlated after application of ORG (Fig. 5*F*; $n = 10$; 5 min: $R = 0.90$, $P < 0.001$; 10 min: $R = 0.85$, $P < 0.01$; Pearson's linear regression).

The increase in I_{HOLD} after application of ORG (I_{ORG}) in GABA-d neurons ($n = 6$) was smaller than that in Gly-d neurons ($n = 4$) before (Fig. 5*G* left columns, $P < 0.05$, unpaired *t* test) and after normalization by cell capacitance (Fig. 5*G* right columns, $P < 0.05$, unpaired *t* test). To test whether tonic GlyR-mediated conductance depends on the degree of basal synaptic release of glycine after application of ORG, amplitudes of I_{ORG} were plotted against basal glycinergic mIPSC frequency. After ORG application, I_{ORG} (Fig. 5*H*; $n = 10$; 5 min: $R = 0.76$, $P < 0.05$; 10 min: $R = 0.75$, $P < 0.05$; Pearson's linear regression) and S.D. of I_{HOLD} (Supplemental Fig. 3*B*; $n = 10$; 5 min: $R = 0.81$, $P < 0.01$; 10 min: $R = 0.70$, $P < 0.05$; Pearson's linear regression) were well correlated with the glycinergic mIPSC frequency. These data suggest that under baseline conditions in spinal cord slices from 3W mice, normally strong activity of GlyT1 near Gly-d neurons made the size of tonic GlyR mediated conductance in Gly-d neurons equal to that in GABA-d neurons. Under basal conditions, I_{tgly} was not dependent on the degree of synaptic activity but became so after inhibition of GlyT1 (compare Fig. 4*H* and 5*H*).

Tonic glycine and $GABA_A$ receptor-mediated conductances in EGFP+ neurons from mature mice

Miniature IPSC frequency changes dramatically over the first two postnatal weeks in rat dorsal horn (Baccei & Fitzgerald, 2004) along with other aspects of synaptic inhibition that continue to change up to postnatal day 30 (Keller *et al.* 2001). The extent of tonic inhibition through $GABA_A$Rs in adult rat dorsal horn neurons is proportional to GABAergic inhibitory synaptic activity (Ataka & Gu, 2006). Therefore, in EGFP+ neurons, it may be that tonic inhibition depends on the properties of synaptic inhibitory inputs and that these properties change developmentally. Moreover, past reports proposed the idea that tonic conductance mediated by GlyRs may disappear after maturation (Mitchell *et al.* 2007). To test these possibilities, we investigated GlyR- and $GABA_A$R-mediated tonic conductance in EGFP+ neurons obtained from mature (5W) animals using the same protocols as for 3W animals. Gly-d neurons showed both I_{tgly} and I_{tGABA} (Fig. 6*A* and *B*). Similarly, GABA-d neurons showed both I_{tgly} and I_{tGABA} (Fig. 6*C* and *D*). However, in contrast to the results with 3W mice, the magnitude of tonic inhibition in 5W mice was clearly related to the synaptic inhibitory input properties of the same neurons. In other words, Gly-d ($n = 5$) neurons had a significantly larger I_{tgly} while GABA-d neurons ($n = 5$) had a significantly larger I_{tGABA}. This was true both before (Fig. 6*E* left columns, $P < 0.05$, unpaired *t* test) and after normalization by cell capacitance (Fig. 6*E* right columns, $P < 0.05$, unpaired *t* test).

To further explore the relationship between the properties of synaptic and tonic inhibition, we calculated the ratio for negative charge transfer through tonic GlyR- and $GABA_A$R-mediated conductances (see Methods). The ratio was not different between Gly-d and GABA-d neurons at 3W (Fig. 6*F* left columns, GABA-d; $n = 11$, Gly-d; $n = 7$), but was remarkably different at 5W (Fig. 6*F* right columns, GABA-d; $n = 5$, Gly-d; $n = 5$, $P < 0.01$, two-way ANOVA with Bonferroni's *post hoc* test). Thus in 5W mice, the Gly-d neurons were significantly more modulated by I_{tgly} than I_{tGABA} while the GABA-d neurons were significantly more modulated by I_{tGABA} than I_{tgly}. As a further indication of this sharpening of receptor type mediating inhibitory tonic current, S.D. of I_{HOLD} was decreased in the presence of bicuculline only in GABA-d neurons compared to control (Fig. 6*G*, $n = 5$, $P < 0.01$, one-way ANOVA with Tukey's *post hoc* test) but not in Gly-d neurons. In the presence of bicuculline plus strychnine, S.D. of I_{HOLD} decreased in both GABA-d and Gly-d neurons compared to bicuculline alone (GABA-d; $n = 5$, $P < 0.01$, Gly-d; $n = 5$, $P < 0.001$, one-way ANOVA with Tukey's *post hoc* test).

These data raise the question of whether the glycine-driving I_{tgly} in Gly-d neurons in 5W mice is associated with synaptic release of glycine even though this was not detectable for 3W mice under basal conditions. In 5W mice, the amplitude of I_{tgly} after strychnine application was well correlated with glycinergic mIPSC frequency (Fig. 6*H*, $n = 10$, $R = 0.77$, $P < 0.05$, Pearson's linear regression). This was also true for S.D. of I_{HOLD} (Supplemental Fig. 3*C*, $n = 10$, $R = 0.84$, $P < 0.01$, Pearson's linear regression). These results support the interpretation that tonic inhibition may be driven by synaptic input properties and spontaneous synaptic release of transmitter at 5W. Consistent with results of 3W animals, the changes in I_{HOLD} and S.D. of I_{HOLD} in the presence of bicuculline and bicuculline plus strychnine were correlated (Supplemental Fig. 3*D*,

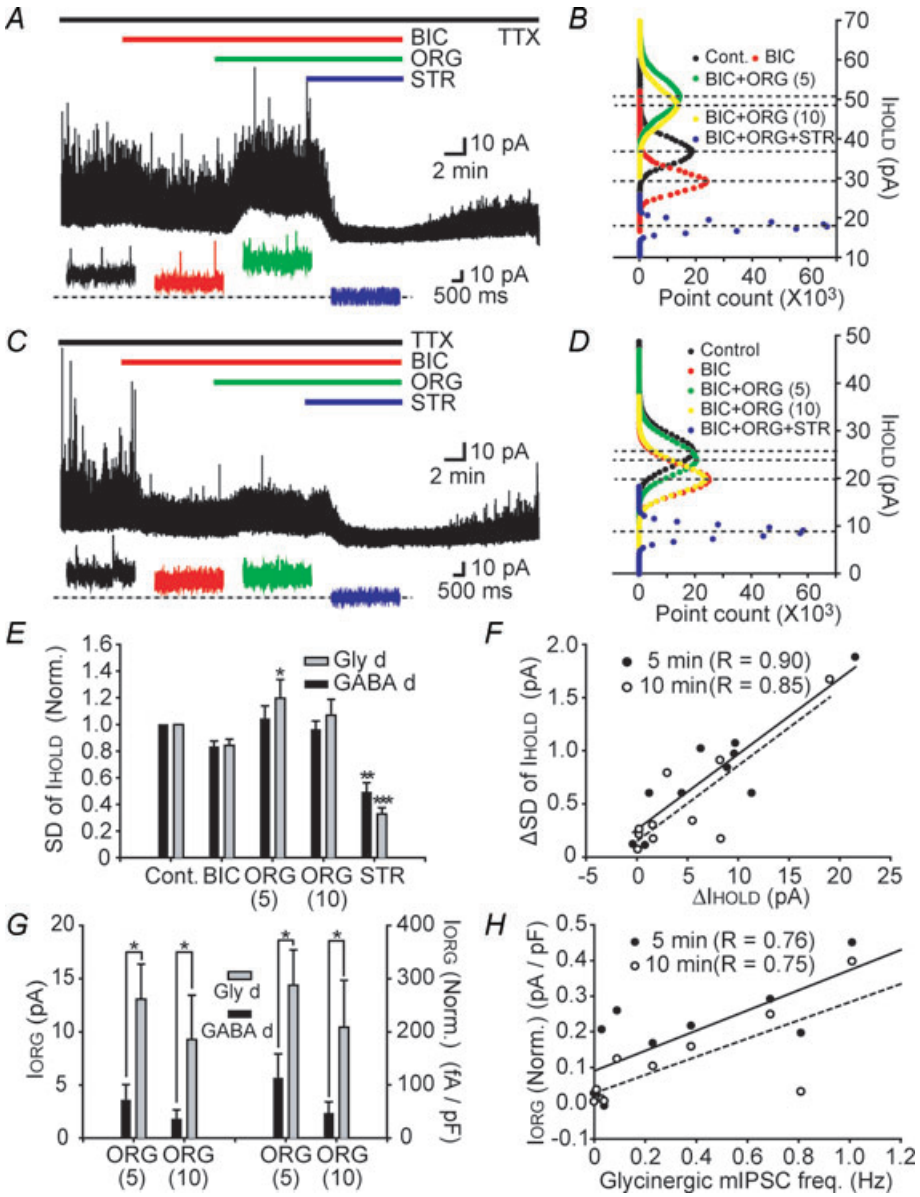

Figure 5. Tonic glycinergic currents were enhanced after application of glycine transporter 1 inhibitor ORG 24598 in both Gly-d and GABA-d EGFP+ neurons

A and *C*, upper traces show baseline shift in Gly-d (*A*) and GABA-d (*C*) neurons induced by bicuculline, followed by co-application with ORG 24598 (ORG; 10 μM) and finally ORG plus strychnine. Expanded time scale traces in lower panel show the shift of holding current (I_{HOLD}) under different conditions. Dotted line indicates I_{HOLD} in the presence of bicuculline, ORG, and strychnine. Holding membrane potential was 0 mV. *B* and *D*, all-points histograms plot the amplitude of I_{HOLD} under different conditions (control, black circles; after application of bicuculline (BIC), red circles; 5 and 10 min after co-application of ORG (BIC+ORG (5) and (10)), green and yellow circles; after co-application of strychnine (BIC+ORG+STR), blue circles). *E*, normalized standard deviation of holding current (SD of I_{HOLD}) was increased after application of ORG in Gly-d ($n = 11$) neurons while it decreased after subsequent co-application of strychnine in the presence of TTX and bicuculline in Gly-d and GABA-d ($n = 7$) neurons. Only statistical differences between subsequent conditions are shown (Tukey's *post hoc* test). *F*, the change in S.D. of I_{HOLD} 5 min (filled circles and continuous line) and 10 min (open circles and dotted line) after application of ORG was well correlated with the change in amplitude of I_{HOLD} after application of ORG ($n = 10$). *G*, left columns, I_{ORG} was greater in Gly-d ($n = 4$) than in GABA-d ($n = 6$) neurons. Right columns, after normalization by cell capacitance, I_{ORG} values were still greater in Gly-d than in GABA-d neurons. *H*, I_{ORG} was well correlated with the basal glycinergic mIPSC frequency 5 min (filled circles and continuous line) and 10 min (open circles and dotted line) after application of ORG ($n = 10$). Data are shown as means ± S.E.M. $^*P < 0.05$, $^{**}P < 0.01$, $^{***}P < 0.001$.

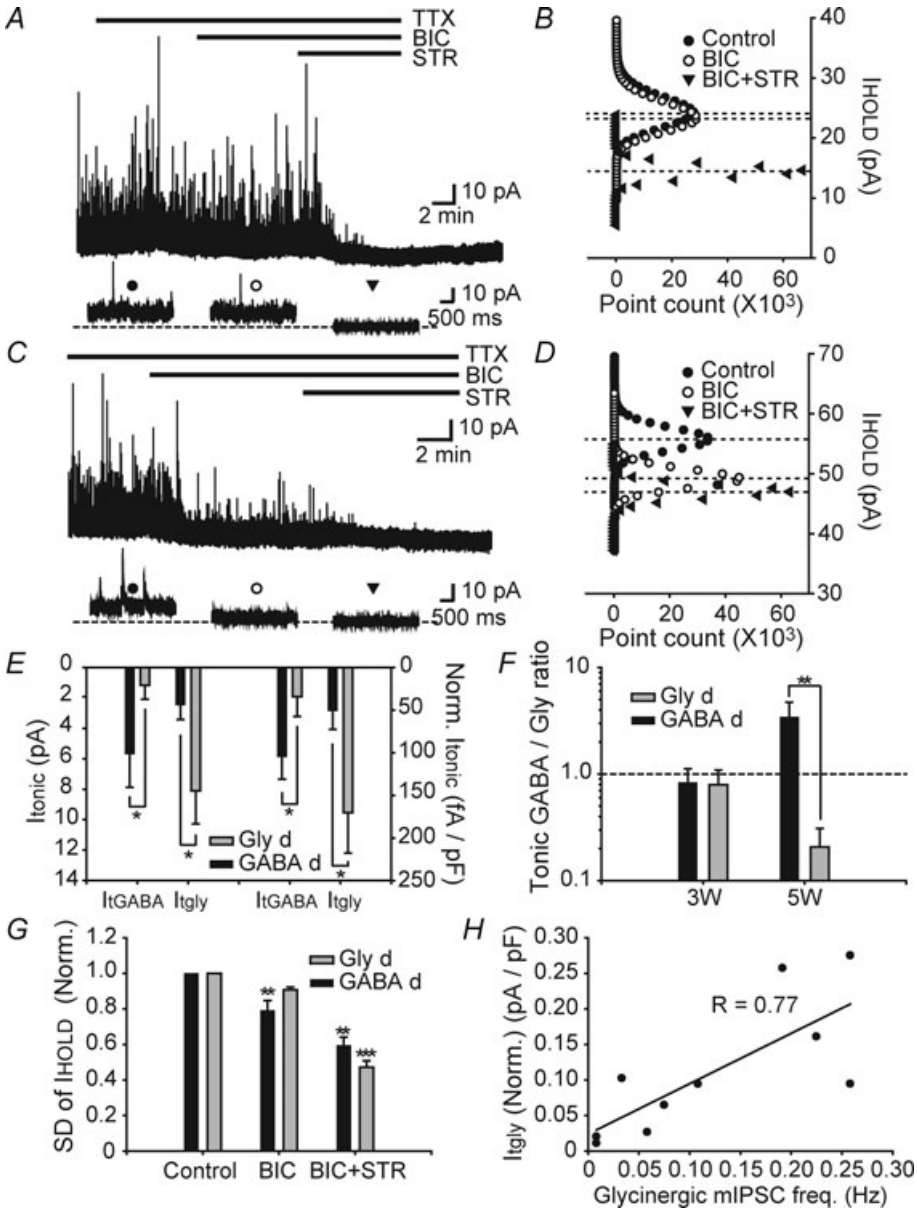

Figure 6. Tonic glycinergic and GABAergic currents in Gly-d and GABA-d EGFP+ neurons obtained from 5W mice

A and *C*, upper traces show bicuculline (BIC) and bicuculline plus strychnine (BIC+STR) induced baseline shift in Gly-d (*A*) and GABA-d neurons (*C*). Expanded time scale traces in lower panel show the shift of holding current (I_{HOLD}) under control (left), BIC (middle), and BIC+STR (right) conditions. Dotted line indicates I_{HOLD} under BIC+STR conditions. Holding membrane potential was 0 mV. *B* and *D*, all-points histograms compare the amplitude of I_{HOLD} under 3 conditions. *E*, both Gly-d neurons ($n = 5$, grey bars) and GABA-d neurons ($n = 5$, black bars) showed I_{tgly} and I_{tGABA}. I_{tgly} was greater in Gly-d than in GABA-d neurons before (left columns) and after normalization by cell capacitance (right columns) *F*, the ratio for negative charge transfer through tonic $GABA_AR$- and GlyR- mediated conductance (Tonic GABA/Gly ratio) was not different between Gly-d (grey bars) and GABA-d (black bars) neurons at 3W (Gly-d; $n = 7$, GABA-d; $n = 11$) but different at 5W (Gly-d, $n = 5$; GABA-d, $n = 5$). *G*, standard deviation of holding current (S.D. of I_{HOLD}) decreased after BIC application only in GABA-d neurons ($n = 5$). S.D. of I_{HOLD} decreased after BIC+STR application in Gly-d ($n = 5$) and GABA-d ($n = 5$) neurons. Only statistical differences between subsequent conditions are shown (one-way ANOVA with Tukey's *post hoc* test). *H*, I_{tgly} was correlated with the basal glycinergic mIPSC frequency ($n = 10$). Data are shown as means ± S.E.M. $^*P < 0.05$, $^{**}P < 0.01$, $^{***}P < 0.001$.

Table 2. Synaptic and tonic charge transfer of the mouse EGFP+ dorsal horn neurons

Age	Glycine/GABA	*n*	Q_{SC} (pC)	Normalized Q_{SC} (pC pF^{-1})	Q_{TC} (pC)	Normalized Q_{TC} (pC pF^{-1})	Q_{TC}/Q_{SC}
3W	Glycine-dominant	7	43 ± 4	0.8 ± 0.1	1790 ± 252*	36.1 ± 8.2	44 ± 6**
	GABA-dominant	11	136 ± 51	3.0 ± 0.9	959 ± 172	27.0 ± 7.4	14 ± 3
5W	Glycine-dominant	5	14 ± 5	0.3 ± 0.1	1114 ± 247	24.6 ± 7.5	97 ± 19***
	GABA-dominant	5	114 ± 65	2.2 ± 1.2	978 ± 311	18.7 ± 4.8	15 ± 4

Q_{SC}, synaptic charge transfer; Q_{TC}, tonic charge transfer. *$P < 0.05$, **$P < 0.01$, ***$P < 0.001$, two-way ANOVA with Bonferroni's *post hoc* test, Gly-d *vs.* GABA-d of same age.

$n = 10$; BIC: $R = 0.93$, $P < 0.0001$; BIC+STR: $R = 0.86$, $P < 0.01$; Pearson's linear regression). Taken together, tonic GlyR- and $GABA_A$R-mediated conductances are preserved in adulthood with a more prominent dependence on inhibitory synaptic input properties, indicating a developmental change in the relationship between synaptic and tonic inhibition.

We next probed the mechanism underlying this dramatic developmental change. I_{tgly} in GABA-d neurons at 5W was much smaller than that at 3W (Compare Fig. 4*G* and 6*E*). This change could be a major factor affecting the ratio for negative charge transfer through tonic GlyR- and $GABA_A$R-mediated conductances (Fig. 6*F*). One possibility is that GlyT1 activity nearby GABA-d neurons may be up-regulated at 5W. Another possibility is that GlyRs responsible for I_{tgly} in GABA-d neurons during maturation become down regulated. To distinguish between these two possibilities, we investigated the effect of ORG in GABA-d neurons at 5W (Supplemental Fig. 4). I_{ORG} at 3W ($n = 6$) and 5W ($n = 4$) were not different before and after normalization by capacitance (Supplemental Fig. 4*C*), suggesting that GlyT1 activity nearby GABA-d neurons was not up-regulated at 5W. Instead, it is likely that GlyRs expressed at GABA-d neurons that are responsible for I_{tgly} were down regulated at 5W.

Comparison of inhibition properties in Gly-d and GABA-d neurons

To directly compare the impact of synaptic and tonic inhibition on neuronal excitability in Gly-d and GABA-d inhibitory neurons, we measured the total negative charge transfer carried by both GlyR- and $GABA_A$R-mediated conductances in a 2 min period of recording (Table 2). After normalizing by cell capacitance, total negative charge transfer through both tonic GlyR- and $GABA_A$R-mediated conductances (Q_{TC}) was not different between GABA-d and Gly-d neurons of both 3W and 5W. Importantly, however, the ratio for inhibitory charge carried by total tonic and synaptic conductance (Q_{TC}/Q_{SC}) was much greater in Gly-d neurons than GABA-d neurons of both 3W and 5W (3W: $P < 0.01$; 5W: $P < 0.001$; two-way ANOVA with Bonferroni's *post hoc* test), although ratios for all populations of inhibitory neurons are considerably greater than 1, suggesting that tonic glycinergic and GABAergic conductances, rather than synaptic conductances, mainly regulate inhibitory tone in EGFP+ neurons throughout 3 to 5W.

Discussion

We have shown that modulation of inhibitory neuron excitability in the spinal cord dorsal horn occurs through tonic inhibition and that the transmitters mediating this tonic inhibition act in a regionally distinct manner. Tonic inhibition is primarily mediated through glycine receptors at the lamina II/III border and through $GABA_A$ receptors in lamina I and IIo. This corresponds well to the dominant transmitter receptor systems mediating spontaneous synaptic transmission in those regions (see Fig. 7). Regional separation of synaptic transmitter action is defined in mice 3 weeks of age but becomes even more distinct by 5 weeks.

Mixed GlyR and $GABA_A$R mIPSCs and synaptic decay τ

Both glycine and GABA are well known as fast inhibitory transmitters in the spinal cord. They have a common vesicular transporter (vesicular inhibitory amino acid transporter; VIAAT) and thus can be loaded into the same synaptic vesicles (Wojcik *et al.* 2006). It follows that when these two transmitters are co-packaged and if both sets of receptors are expressed postsynaptically, spontaneous quantal synaptic events will show a mixture of glycinergic and GABAergic characteristics. However, even when the two transmitters are co-packaged, postsynaptic receptor composition can cause synaptic events to be only glycinergic or GABAergic (Jonas *et al.* 1998; Keller *et al.* 2001; Baccei & Fitzgerald, 2004; Mitchell *et al.* 2007; Rajalu *et al.* 2009). In our studies on GAD67 EGFP+ neurons, analysis of mIPSCs recorded from different neurons showed that just a few neurons received purely glycinergic or GABAergic mIPSCs. This is indicated by the cells in Fig. 2*E* that show no block ($n = 2$) or 100% block ($n = 1$) with bicuculline. Thus most EGFP+

neurons in lamina I–III receive a mixture of GlyR- and $GABA_AR$-mediated mIPSCs, similar to recordings from neurons expressing EGFP driven by the GAD65 promoter in adult mice (Labrakakis *et al.* 2009). However, in our studies, we found that interneurons at the lamina II/III border are glycine dominant and lamina I–IIo interneurons are GABA dominant based on two independent factors: pharmacological sensitivity of mIPSC frequency and mean decay τ (i.e. the time required for the events to decay by 67%). This result is consistent with a recent report concluding that inhibitory synaptic transmission in deeper lamina (III–IV) was characterized by a dominant role for glycinergic inhibition (Inquimbert *et al.* 2007). Immunohistochemical studies showed that expression of GlyR α_1 subunits (a component of the major GlyR isoform in adult spinal cord) gradually increased from dorsal to ventral in dorsal horn (Harvey *et al.* 2004), while $GABA_AR$ β_3 subunits (predominant subunit in spinal neurons) were most dense in lamina I and II (Todd *et al.* 1996), although the distribution pattern of $GABA_ARs$ varied with the different $GABA_AR$ subunits (Bohlhalter *et al.* 1996). This evidence is consistent with our results.

Developmental changes in inhibitory modulation of inhibitory neurons

Regulation of extracellular glycine and GABA concentrations may be a key factor in determining local inhibitory tone in the dorsal horn but the impact of these transmitters may vary with age. Glycine transporters, especially GlyT1, are responsible for removing glycine from the extracellular space, thus playing a key role in controlling local extracellular glycine concentration (Eulenburg *et al.* 2005). While I_{tGABA} has been reported in lamina II neurons from adult mice (Ataka & Gu, 2006), I_{tgly} has only been reported in lamina II neurons from juvenile rats (2–3 weeks postnatal) (Mitchell *et al.* 2007). It was suggested that I_{tgly} may disappear developmentally after that age, accounting for why it was not previously reported in dorsal horn neurons (Mitchell *et al.* 2007).

Our observations on inhibitory neurons, especially those at the lamina II/III border, show I_{tgly} is expressed not only by juvenile mice but also by mature mice of 5W. In agreement with previous reports (Bradaia *et al.* 2004; Mitchell *et al.* 2007), we found that blockade of GlyT1 activity caused an outward shift in the holding current accompanied by an increase in S.D. of I_{HOLD} (Fig. 5), supporting the existence of tonic-GlyR mediated conductance in 3W animals. In 5W mice, I_{tgly} had diminished considerably in lamina I and IIo GAD67 EGFP+ neurons, which are mostly GABA-d (compare Figs 4*G* and 6*E*), while it remained prominently expressed at lamina II/III border, mostly Gly-d, neurons (compare Figs 4*G* and 6*E*). Thus in our experiments, I_{tGly} diminished developmentally as suggested by Mitchell *et al.* (2007) but only in GABA-d neurons and not in Gly-d neurons. It may be that I_{tgly} was not previously observed in adult mouse dorsal horn (Ataka & Gu, 2006) because I_{tgly} is so small in GABA-d neurons at 5W and because Gly-d neurons, in which it is pronounced, are relatively ventrally located in lamina II and thus may not have been studied.

In the present study, we suggest that down-regulation of GlyRs is responsible for the decrease in I_{tgly} in GABA-d neurons at 5W (Supplemental Fig. 4). In addition, I_{tGABA} in Gly-d neurons decreased developmentally (compare Figs 4*G* and 6*E*), suggesting that $GABA_ARs$ responsible for I_{tGABA} may be down-regulated. Another possibility is that GABA transporter activity becomes up regulated near Gly-d neurons. Taken together, developmental changes in inhibitory systems, including down regulation of GlyRs responsible for I_{tgly} in GABA-d neurons, make the relationship with synaptic and tonic inhibition on inhibitory neurons more prominent in fully mature mice.

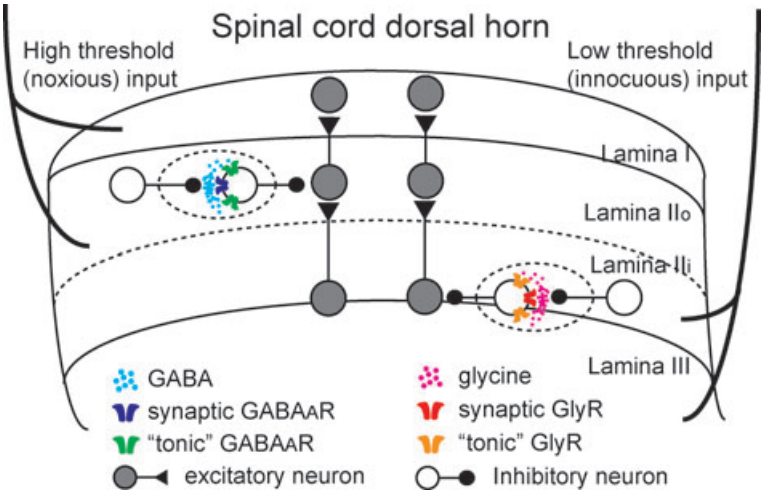

Figure 7. Regionally distinct subpopulations of inhibitory dorsal horn neurons were modulated through different synaptic and extrasynaptic receptors
Dotted circles indicate the focus of the current study: how inhibitory neuron excitability is modulated by local circuitry. Inhibitory neurons at lamina II/III border predominantly receive glycinergic synaptic and tonic inhibition. Lamina I and IIo inhibitory neurons, in contrast, predominantly receive GABAergic synaptic and tonic inhibition. This schematic diagram was drawn on the basis of our results obtained from 5-week-old mice. Different symbols for synaptic and 'tonic' receptors do not necessarily mean distinct subtypes of receptors.

Inhibitory tone modulates inhibitory neuronal excitability in the dorsal horn

Conventionally, synaptic rather than tonic inhibition has been assumed to be the main regulator for inhibitory tone in neuron networks. Indeed, strong synaptic inhibitory drive has been demonstrated in the dorsal horn. For example, lamina II neurons receiving primary afferent excitation also receive closely timed disynaptic inhibition (Yoshimura & Nishi, 1995), suggesting that synaptic inhibitory input synchronized with incoming excitatory input plays a critical role influencing neuronal excitability when the neuron receives evoked excitatory input. Tonic inhibition through GlyR- and $GABA_A$R-mediated conductances limits neuronal excitability of inhibitory neurons in a manner that is less precisely timed. Given that the total negative charge carried by tonic conductance was much greater than that by spontaneous synaptic conductance (Table 2), tonic inhibition may have a pivotal role in regulating inhibitory neuronal excitability in the dorsal horn.

We showed that disinhibition by pharmacological blockade of glycinergic and GABAergic receptors with antagonists caused enhanced neuronal excitability in GAD67 EGFP+ neurons (Fig. 1). Inhibition of GlyR and $GABA_A$R produced a leftward shift of the curves for *F–I* relationships along the current axis indicating a subtractive effect rather than a change of gain of the curve, as has been predicted by theoretical models (Holt & Koch, 1997; Chance *et al.* 2002). Although our stimulation (i.e. tonic excitation with current step injection) is not an endogenous physiological stimulus, the results are consistent with past reports testing similar excitation in other CNS neurons (Brickley *et al.* 1996; Hamann *et al.* 2002; Ulrich, 2003) and suggest that tonic inhibition was a major source of suppressed excitability in the absence of glycine and GABA antagonists. It is important to keep in mind, however, that our comparison of the impact of spontaneous synaptic and tonic inhibition on neuronal excitability is based on data obtained from isolated slice preparations lacking action potential driven synaptic inputs from peripheral fibres and CNS regions. Thus, our data do not necessarily mean that tonic inhibition always has greater impact on neuronal excitability than synaptically driven inhibition *in vivo*.

Significance of regional differences in inhibitory tone

Functionally, laminae I and IIo in the dorsal horn are quite distinct from lamina IIi and III in terms of sensory modality. Laminae I and II are typically innervated by pain-, temperature- and itch-carrying primary afferents while deep lamina IIi and lamina III receive input from touch-carrying afferents (Fig. 7). Nevertheless, the low threshold inputs to the lamina II/III border may be able to penetrate to normally high threshold fibre driven, lamina I projection neurons by way of a polysynaptic excitatory pathway under conditions of disinhibition (Torsney & MacDermott, 2006). A recent study showed that PKCγ positive neurons in lamina IIi are key elements for circuits activated after disinhibition by GlyR antagonist. These drugs induce a dynamic form of mechanical allodynia by unmasking usually blocked local circuits onto lamina I, nociceptive output neurons (Miraucourt *et al.* 2007). Given that most inhibitory neurons in laminae I and II are located at the same dorso-ventral level as their post-synaptic target neurons (Kato *et al.* 2009), inhibitory neurons located at the lamina II/III border receiving glycinergic synaptic inputs (Fig. 3) and GlyR-mediated tonic inhibition (Supplemental Fig. 5), may inhibit PKCγ positive neurons directly. Thus glycinergic inhibitory modulation of glycinergic inhibitory neurons is expected to provide dynamic regulation of this gateway between touch and pain.

Tonic inhibition may be modified under pathological conditions because several factors released into the spinal cord following inflammation and peripheral injury can modulate GABA and glycine transporter activity (Patrylo *et al.* 2001; Eulenburg *et al.* 2005). For example, arachidonic acid inhibits GlyT1 (Zafra *et al.* 1990; Pearlman *et al.* 2003), suggesting that extracellular glycine concentration could be higher under inflammatory conditions. In that situation, the activity of inhibitory neurons particularly at the lamina II/III border would be decreased because those neurons have substantial glycinergic inhibitory conductance. Thus, inflammation, acting through tonic inhibition, could cause a change of the balance between excitatory and inhibitory signals modulating dorsal horn neuronal excitability.

References

Ataka T & Gu JG (2006). Relationship between tonic inhibitory currents and phasic inhibitory activity in the spinal cord lamina II region of adult mice. *Mol Pain* **2**, 36.

Baccei ML & Fitzgerald M (2004). Development of GABAergic and glycinergic transmission in the neonatal rat dorsal horn. *J Neurosci* **24**, 4749–4757.

Bai D, Zhu G, Pennefather P, Jackson MF, MacDonald JF & Orser BA (2001). Distinct functional and pharmacological properties of tonic and quantal inhibitory postsynaptic currents mediated by γ-aminobutyric $acid_A$ receptors in hippocampal neurons. *Mol Pharmacol* **59**, 814–824.

Beato M (2008). The time course of transmitter at glycinergic synapses onto motoneurons. *J Neurosci* **28**, 7412–7425.

Bohlhalter S, Weinmann O, Mohler H & Fritschy JM (1996). Laminar compartmentalization of $GABA_A$-receptor subtypes in the spinal cord: an immunohistochemical study. *J Neurosci* **16**, 283–297.

Bradaia A, Schlichter R & Trouslard J (2004). Role of glial and neuronal glycine transporters in the control of glycinergic and glutamatergic synaptic transmission in lamina X of the rat spinal cord. *J Physiol* **559**, 169–186.

Brickley SG, Cull-Candy SG & Farrant M (1996). Development of a tonic form of synaptic inhibition in rat cerebellar granule cells resulting from persistent activation of $GABA_A$ receptors. *J Physiol* **497**, 753–759.

Brickley SG, Revilla V, Cull-Candy SG, Wisden W & Farrant M (2001). Adaptive regulation of neuronal excitability by a voltage-independent potassium conductance. *Nature* **409**, 88–92.

Chance FS, Abbott LF & Reyes AD (2002). Gain modulation from background synaptic input. *Neuron* **35**, 773–782.

Chery N & de Koninck Y (1999). Junctional versus extrajunctional glycine and $GABA_A$ receptor-mediated IPSCs in identified lamina I neurons of the adult rat spinal cord. *J Neurosci* **19**, 7342–7355.

Daniele CA & MacDermott AB (2009). Low-threshold primary afferent drive onto GABAergic interneurons in the superficial dorsal horn of the mouse. *J Neurosci* **29**, 686–695.

Debarbieux F, Brunton J & Charpak S (1998). Effect of bicuculline on thalamic activity: a direct blockade of I_{AHP} in reticularis neurons. *J Neurophysiol* **79**, 2911–2918.

Dougherty KJ, Sawchuk MA & Hochman S (2005). Properties of mouse spinal lamina I GABAergic interneurons. *J Neurophysiol* **94**, 3221–3227.

Eulenburg V, Armsen W, Betz H & Gomeza J (2005). Glycine transporters: essential regulators of neurotransmission. *Trends Biochem Sci* **30**, 325–333.

Farrant M & Nusser Z (2005). Variations on an inhibitory theme: phasic and tonic activation of $GABA_A$ receptors. *Nat Rev* **6**, 215–229.

Gomeza J, Hulsmann S, Ohno K, Eulenburg V, Szoke K, Richter D & Betz H (2003). Inactivation of the glycine transporter 1 gene discloses vital role of glial glycine uptake in glycinergic inhibition. *Neuron* **40**, 785–796.

Hamann M, Rossi DJ & Attwell D (2002). Tonic and spillover inhibition of granule cells control information flow through cerebellar cortex. *Neuron* **33**, 625–633.

Hantman AW, Van Den Pol AN & Perl ER (2004). Morphological and physiological features of a set of spinal substantia gelatinosa neurons defined by green fluorescent protein expression. *J Neurosci* **24**, 836–842.

Harvey RJ, Depner UB, Wassle H, Ahmadi S, Heindl C, Reinold H, Smart TG, Harvey K, Schutz B, Abo-Salem OM, Zimmer A, Poisbeau P, Welzl H, Wolfer DP, Betz H, Zeilhofer HU & Muller U (2004). GlyR α3: an essential target for spinal PGE2-mediated inflammatory pain sensitization. *Science* **304**, 884–887.

Heaulme M, Chambon JP, Leyris R, Wermuth CG & Biziere K (1987). Characterization of the binding of [^{3}H]SR 95531, a $GABA_A$ antagonist, to rat brain membranes. *J Neurochem* **48**, 1677–1686.

Heinke B, Ruscheweyh R, Forsthuber L, Wunderbaldinger G & Sandkuhler J (2004). Physiological, neurochemical and morphological properties of a subgroup of GABAergic spinal lamina II neurones identified by expression of green fluorescent protein in mice. *J Physiol* **560**, 249–266.

Holt GR & Koch C (1997). Shunting inhibition does not have a divisive effect on firing rates. *Neural Comput* **9**, 1001–1013.

Inquimbert P, Rodeau JL & Schlichter R (2007). Differential contribution of GABAergic and glycinergic components to inhibitory synaptic transmission in lamina II and laminae III–IV of the young rat spinal cord. *Eur J Neurosci* **26**, 2940–2949.

Jonas P, Bischofberger J & Sandkuhler J (1998). Corelease of two fast neurotransmitters at a central synapse. *Science* **281**, 419–424.

Kato G, Kawasaki Y, Koga K, Uta D, Kosugi M, Yasaka T, Yoshimura M, Ji RR & Strassman AM (2009). Organization of intralaminar and translaminar neuronal connectivity in the superficial spinal dorsal horn. *J Neurosci* **29**, 5088–5099.

Keller AF, Coull JA, Chery N, Poisbeau P & De Koninck Y (2001). Region-specific developmental specialization of GABA-glycine cosynapses in laminas I-II of the rat spinal dorsal horn. *J Neurosci* **21**, 7871–7880.

Khawaled R, Bruening-Wright A, Adelman JP & Maylie J (1999). Bicuculline block of small-conductance calcium-activated potassium channels. *Pflugers Arch* **438**, 314–321.

Labrakakis C, Lorenzo LE, Bories C, Ribeiro-da-Silva A & De Koninck Y (2009). Inhibitory coupling between inhibitory interneurons in the spinal cord dorsal horn. *Mol Pain* **5**, 24.

Light AR & Perl ER (1979). Reexamination of the dorsal root projection to the spinal dorsal horn including observations on the differential termination of coarse and fine fibres. *J Comp Neurol* **186**, 117–131.

Melzack R & Wall PD (1965). Pain mechanisms: a new theory. *Science* **150**, 971–979.

Miraucourt LS, Dallel R & Voisin DL (2007). Glycine inhibitory dysfunction turns touch into pain through PKCγ interneurons. *PLoS ONE* **2**, e1116.

Mitchell EA, Gentet LJ, Dempster J & Belelli D (2007). $GABA_A$ and glycine receptor-mediated transmission in rat lamina II neurones: relevance to the analgesic actions of neuroactive steroids. *J Physiol* **583**, 1021–1040.

Mtchedlishvili Z & Kapur J (2006). High-affinity, slowly desensitizing $GABA_A$ receptors mediate tonic inhibition in hippocampal dentate granule cells. *Mol Pharmacol* **69**, 564–575.

Oliva AA Jr, Jiang M, Lam T, Smith KL & Swann JW (2000). Novel hippocampal interneuronal subtypes identified using transgenic mice that express green fluorescent protein in GABAergic interneurons. *J Neurosci* **20**, 3354–3368.

Park JB, Skalska S & Stern JE (2006). Characterization of a novel tonic γ-aminobutyric acidA receptor-mediated inhibition in magnocellular neurosecretory neurons and its modulation by glia. *Endocrinology* **147**, 3746–3760.

Patrylo PR, Spencer DD & Williamson A (2001). GABA uptake and heterotransport are impaired in the dentate gyrus of epileptic rats and humans with temporal lobe sclerosis. *J Neurophysiol* **85**, 1533–1542.

Pearlman RJ, Aubrey KR & Vandenberg RJ (2003). Arachidonic acid and anandamide have opposite modulatory actions at the glycine transporter, GLYT1a. *J Neurochem* **84**, 592–601.

Rajalu M, Muller UC, Caley A, Harvey RJ & Poisbeau P (2009). Plasticity of synaptic inhibition in mouse spinal cord lamina II neurons during early postnatal development and after inactivation of the glycine receptor α3 subunit gene. *Eur J Neurosci* **30**, 2284–2292.

Reinold H, Ahmadi S, Depner UB, Layh B, Heindl C, Hamza M, Pahl A, Brune K, Narumiya S, Muller U & Zeilhofer HU (2005). Spinal inflammatory hyperalgesia is mediated by prostaglandin E receptors of the EP2 subtype. *J Clin Invest* **115**, 673–679.

Semyanov A, Walker MC, Kullmann DM & Silver RA (2004). Tonically active $GABA_A$ receptors: modulating gain and maintaining the tone. *Trends Neurosci* **27**, 262–269.

Seutin V, Scuvee-Moreau J & Dresse A (1997). Evidence for a non-GABAergic action of quaternary salts of bicuculline on dopaminergic neurones. *Neuropharmacology* **36**, 1653–1657.

Sherman SE & Loomis CW (1996). Strychnine-sensitive modulation is selective for non-noxious somatosensory input in the spinal cord of the rat. *Pain* **66**, 321–330.

Sivilotti L & Woolf CJ (1994). The contribution of $GABA_A$ and glycine receptors to central sensitization: disinhibition and touch-evoked allodynia in the spinal cord. *J Neurophysiol* **72**, 169–179.

Sorkin LS & Puig S (1996). Neuronal model of tactile allodynia produced by spinal strychnine: effects of excitatory amino acid receptor antagonists and a mu-opiate receptor agonist. *Pain* **68**, 283–292.

Stell BM & Mody I (2002). Receptors with different affinities mediate phasic and tonic $GABA_A$ conductances in hippocampal neurons. *J Neurosci* **22**, RC223.

Takahashi A, Mashimo T & Uchida I (2006). GABAergic tonic inhibition of substantia gelatinosa neurons in mouse spinal cord. *Neuroreport* **17**, 1331–1335.

Todd AJ & Sullivan AC (1990). Light microscope study of the coexistence of GABA-like and glycine-like immunoreactivities in the spinal cord of the rat. *J Comp Neurol* **296**, 496–505.

Todd AJ, Watt C, Spike RC & Sieghart W (1996). Colocalization of GABA, glycine, and their receptors at synapses in the rat spinal cord. *J Neurosci* **16**, 974–982.

Torsney C & MacDermott AB (2006). Disinhibition opens the gate to pathological pain signalling in superficial neurokinin 1 receptor-expressing neurons in rat spinal cord. *J Neurosci* **26**, 1833–1843.

Ulrich D (2003). Differential arithmetic of shunting inhibition for voltage and spike rate in neocortical pyramidal cells. *Eur J Neurosci* **18**, 2159–2165.

Wojcik SM, Katsurabayashi S, Guillemin I, Friauf E, Rosenmund C, Brose N & Rhee JS (2006). A shared vesicular carrier allows synaptic corelease of GABA and glycine. *Neuron* **50**, 575–587.

Yaksh TL (1989). Behavioural and autonomic correlates of the tactile evoked allodynia produced by spinal glycine inhibition: effects of modulatory receptor systems and excitatory amino acid antagonists. *Pain* **37**, 111–123.

Yeung JY, Canning KJ, Zhu G, Pennefather P, MacDonald JF & Orser BA (2003). Tonically activated $GABA_A$ receptors in hippocampal neurons are high-affinity, low-conductance sensors for extracellular GABA. *Mol Pharmacol* **63**, 2–8.

Yoshimura M & Nishi S (1995). Primary afferent-evoked glycine- and GABA-mediated IPSPs in substantia gelatinosa neurones in the rat spinal cord *in vitro*. *J Physiol* **482**, 29–38.

Zafra F, Alcantara R, Gomeza J, Aragon C & Gimenez C (1990). Arachidonic acid inhibits glycine transport in cultured glial cells. *Biochem J* **271**, 237–242.

Author contributions

T.T. planned, performed and analysed the experiments, and wrote the initial draft of the paper. A.B.M contributed to experimental design and to writing the paper.

Acknowledgements

We thank Yukio Koyama for providing software for analysis. We thank Steven Siegelbaum and Gregory Scherrer for helpful comments on the manuscript. This work was supported by NIH R01 NS 029797.